Reports

High-Pressure Physics: Sustained Static Generation of 1.36 to 1.72 Megabars

Abstract. *The pressure in experiments with the diamond-window pressure cell exceeded 1.7 megabars (at 25°C). This is the highest sustained pressure ever generated under static conditions where the pressure in the sample itself was measured. At 1.72 megabars, macroscopic flow of one of the diamond pressure faces was observed.*

The first experiments in which a static pressure of 1.72 Mbar was generated at room temperature (25°C) are reported here. Measurements of the pressure were made directly on ruby crystals in the pressurized medium itself.

In earlier experiments to 1 Mbar (*1*), pressure measurements were based on an extension of the National Bureau of Standards calibration scale for the pressure dependence of the ruby R_1 fluorescence (*2*). More recently, this extension of the ruby R_1 scale has been calibrated from 0.06 to 1.0 Mbar (*3*). The calibration experiments were done by studying the volume changes of the four metals Cu, Mo, Pd, and Ag simultaneously under pressure, using x-ray diffraction through the pressure cell. Pressure-volume relations for these metals are well known from accurate shock wave experiments in which the errors and uncertainties are negligible. Ruby crystals were embedded in the composite metal sample so that the ruby fluorescence wavelength shift with pressure could be correlated directly with the pressure-volume relations. The results of this recent calibration indicated that there is a small positive nonlinearity in the pressure dependence of the wavelength shift, but the deviation from the reported pressure at 1 Mbar was within the estimated uncertainty (± 10 percent of pressure). In the work reported here pressure was measured by using an extension of the resulting R_1 pressure scale to 1 Mbar given by

$$P = 3.808[(\Delta\lambda/694.2 + 1)^5 - 1]$$

where pressure is in megabars and $\Delta\lambda$ (nanometers) is the wavelength shift of the ruby R_1 fluorescence line between 1 bar and the high pressure.

The apparatus used in these experiments was the diamond-window pressure cell (*2*). The windows were made of 0.3-carat brilliant-cut diamonds whose culet tips were ground flat or beveled in part to low angles (see Fig. 1). Diamonds with low strain birefringence (2 to 10 × 10^{-5}) were selected.

The alignment cylinders [which also act as thrust blocks in the pressure cell (*4*)] were cast of tungsten carbide, complete with access ports to the diamond windows (by the Metallurgy Division, General Electric Company), except for experiment 6C1, in which the ports were

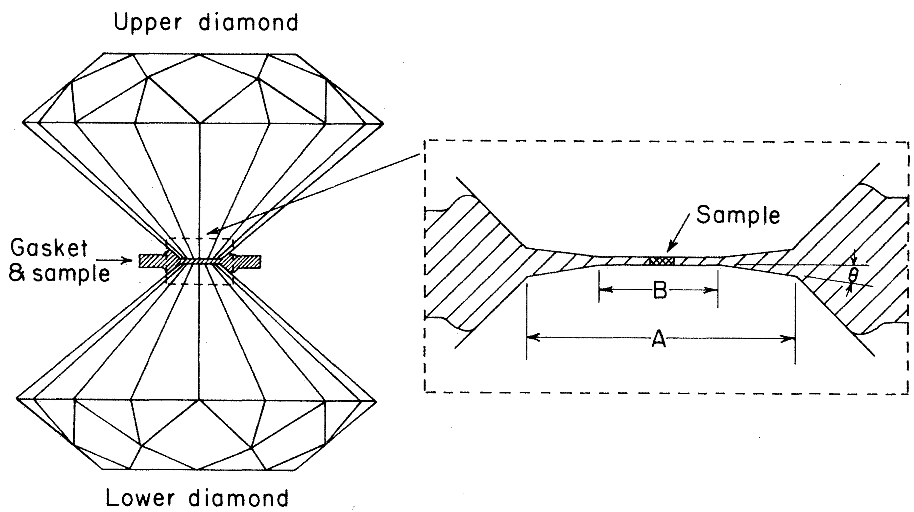

Fig. 1. Sketch of the diamond-window pressure cell (distance from top surface of upper diamond to bottom surface of lower diamond, approximately 5 mm). (Inset) Magnified view of a cross section of the gasket-sample assembly; A, outer diameter of the bevel; θ, the bevel angle; and B, the flat surface; the sample width is 250 μm.

Table 1. Orientation, strain, and dimensional parameters of the diamond windows.

Observation	6Cl		13Cl		13C2		13C3	
	Upper window*	Lower window*	Upper window	Lower window	Upper window	Lower window	Upper window	Lower window
Orientation†	(100)	Random‡	(510)	(100)	(111)	(111)	(741)	(100)
Maximum strain								
Birefringence (× 10^{-5})	N.D.§	N.D.	10	6	10	2	6	6
A (mm)	0.66	0.66	0.37	0.34	0.26	0.25	0.30	0.29
B (mm)	0.25	0.23	0.15				0.18	0.18
θ (degrees)	2	2	2	0	0	0	2	1
Maximum pressure (Mbar)	1.55		1.36		1.43		1.72	
Damage at maximum pressure								
To window	Split	Crushed	Crushed	Chipped‖	Crushed	Chipped‖	Flowed	None
To carbide seat	Cracked	Cracked	None	None	None	None	None	None

*The upper diamond was mounted on the cylinder, the lower diamond on the piston. †Miller indices of the anvil face. ‡Not close to (100), (110), or (111). §N.D., not determined. ‖Anvil face slightly chipped at the shock of crushing the other diamond.

0036-8075/78/0609-1145$00.50/0

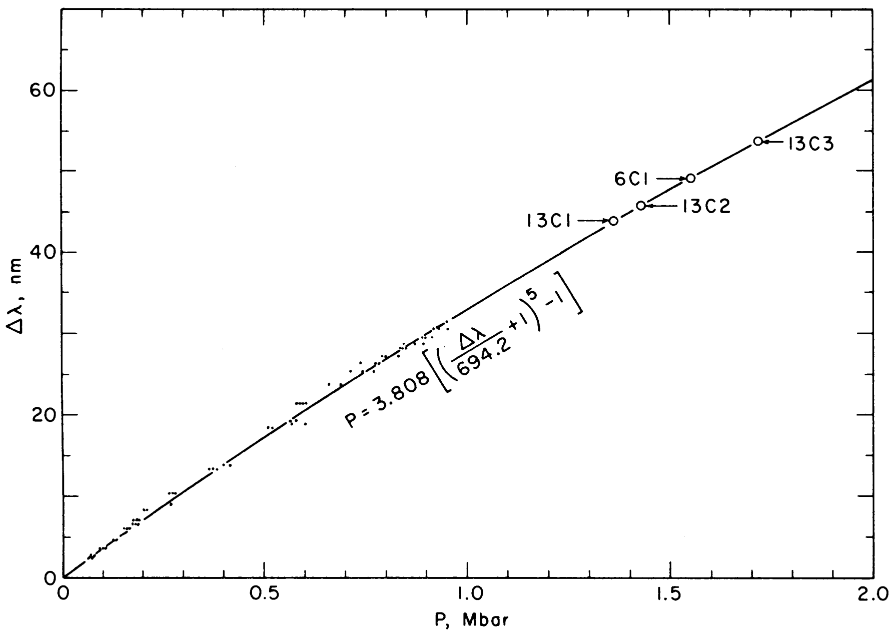

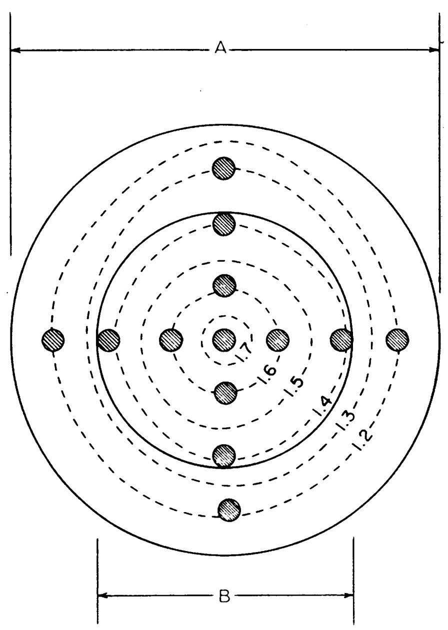

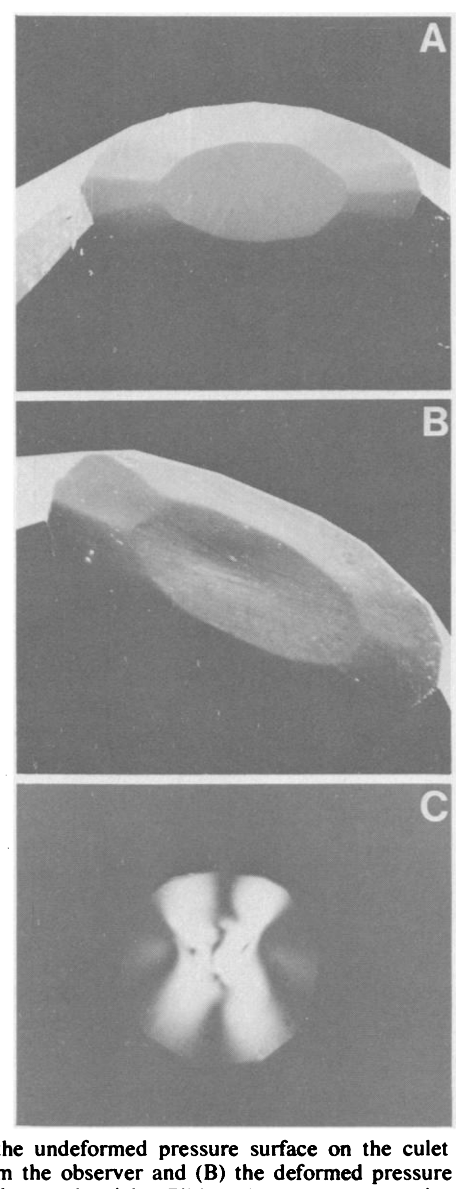

Fig. 2 (top). Wavelength of the ruby R_1 fluorescence line plotted against pressure. Solid points are calibration points based on equation-of-state measurements of Cu, Mo, Ag, and Pd from shock wave data (3). Solid line is a nonlinear, three-parameter, least-squares fit to the calibration points. Numbered open circles are the maximum pressures measured in the present study. Fig. 3 (above left). Pressure contours (in megabars) on the upper diamond pressure face in experiment 13C3. Measurements of the ruby R_1 fluorescence line were made at points indicated by the shaded circles (diameter of the He-Cd laser beam). Solid circular lines mark the edge of the bevel (A, 300 μm; B, 180 μm). Fig. 4 (bottom right). Photomicrographs of flow deformation observed on the upper diamond face in experiment 13C3 after the maximum pressure of 1.72 Mbar was unloaded to 1 bar. (A and B) Scanning electron micrographs (backscattered electron image) showing (A) the undeformed pressure surface on the culet tip of the diamond in a view tilted away from the observer and (B) the deformed pressure surface at higher magnification and tilted farther to the right. Tilting gives oval perspective illusion. Note the bevel and the flow deformation in the central portions. (C) Light photomicrograph of the diamond under cross polarization viewed normal to the plane of the pressure face. Interference bands converge toward the center, where maximum deformation is observed.

"drilled" by the electroetching technique. High-precision alignment of the diamonds was achieved by measuring pressure gradients at 700 kbar with the fluorescence shift of ruby crystals that were distributed radially in the cell. Adjustments were made so that these gradients were symmetrical with respect to the center of the diamond culet faces.

The sample assembly consisted of a preindented gasket made of work-hardened stainless steel, on the upper surface of which ruby crystals were embedded (Fig. 1). During the experiments the ruby R_1 fluorescence line was excited by probing the sample with a He-Cd laser beam focused through the diamond window (5). The pressure was raised from 700 kbar at 25°C (after the alignment described above) to the pressures on the calibration curve indicated by arrows in Fig. 2. Pressures were measured at every 50- to 100-kbar increment in the entire range from 1 bar to the maximum pressure. At the highest pressure, the pressure distribution on the diamond faces was contoured with data from the ruby fluorescence measurements at various points, as shown in the example in Fig. 3.

The maximum pressure reading obtained was 1.72 Mbar (the systematic uncertainty in pressure above the calibrated point at 1 Mbar is estimated to be + 20 percent, − 10 percent). In that experiment, a color change was observed at the center of the diamond pressure face (within the 1.7-Mbar contour; Fig. 3) from colorless to a light shade of brown, which might indicate the onset of a phase transformation (discounting possible hysteresis of the presumed transformation) or of deformation. Further applications of force caused no increase in pressure, so the experiment was terminated. The cell was left undisturbed for 18 hours, during which the pressure remained constant at 1.7 Mbar. Pressure was gradually released to 1 bar (over 5 hours) to avoid possible cracking of the diamonds. The brown coloration referred to above persisted until the pressure was reduced to 1.0 Mbar. Between 1.0 and 0.8 Mbar the brown completely disappeared, and the observed diamond pressure face returned to its colorless state. Examination of the diamonds by microscope on release of pressure revealed no obvious cracks, but relatively massive flow deformation was observed for the first time at these pressures (6) in the upper diamond along its pressure face in the same region that had turned brown. The flat B area of the upper diamond (Fig. 1) became permanently concave (Fig. 4, A and B). Also, the strain in the central area of the anvil increased markedly (Fig. 4C). The maximum birefringence increased from the initial 6×10^{-5} to 6×10^{-3}. The lower diamond showed no visual indication of flow or other deformation. Its strain birefringence was unchanged.

In addition to the 1.72-Mbar experiment, Table 1 lists details of experiments in which the maximum pressures were 1.36, 1.43, and 1.55 Mbar. These experiments were terminated because of sudden failure of one of the diamonds in each instance. Although diamond failure appears to be a random process, the fact that one of the diamonds used in the 1.72-Mbar experiment did not flow or fail suggests that it may be possible to generate pressures higher than this.

The pressure of 1.7 Mbar is the highest sustained static pressure ever achieved experimentally. This maximum pressure is almost 3.5 times higher than the highest pressures reported by other laboratories in which continuous internal calibration was employed (*7*). The depth in the earth that corresponds to a pressure of 1.7 Mbar is approximately 3000 km (*8*) and is within the earth's core. The techniques described here can be applied to geophysical problems under conditions simulating those of the core-mantle boundary, as well as to a wide range of physical or chemical experiments on the nature of matter.

H. K. MAO
P. M. BELL

*Geophysical Laboratory,
Carnegie Institution of Washington,
Washington, D.C. 20008*

References and Notes

1. The sample in all these experiments is a composite of ruby crystals embedded in full-hardened T301 stainless steel.
2. H. K. Mao and P. M. Bell, *Science* **191**, 851 (1976).
3. ———, J. Shaner, D. Steinberg, *J. Appl. Phys.*, in press.
4. H. K. Mao and P. M. Bell, *Carnegie Inst. Washington Yearb.* **74**, 402 (1975).
5. The beam of an RCA He-Cd laser (441 mm) was focused to 20 μm.
6. T. Evans and R. K. Wild, *Philos. Mag.* **12**, 419 (1965).
7. The U.S. National Bureau of Standards reported 0.5 Mbar; see G. J. Piermarini and S. Block, *Rev. Sci. Instrum.* **46**, 973 (1975).
8. S. P. Clark, Jr., and A. E. Ringwood, *Rev. Geophys.* **2**, 35 (1964).
9. We thank instrument makers C. A. Batten, J. Schwartz, and C. Brown for constructing the 1.7-Mbar pressure cell. We gratefully acknowledge the support of NSF grant EAR 76-81703 in addition to that of the Carnegie Institution of Washington. The diamonds employed in this study were supplied, cut and ground, by Double D Diamond Corp. and Lazare Kaplan & Sons Inc., New York.

7 April 1978

Chytrid-Like Fossils of Pennsylvanian Age

Abstract. *Chytrid-like fungal sporangia are described occurring in saccate pollen grains of Pennsylvanian age. Both endo- and epibiotic sporangia are present, and may exhibit discharge papillae and a coarse rhizomycelium. Sporangial features, choice of substrate, and the presence of a light refractile body in presumed zoospores suggest relationships with the Chytridiales.*

There are a number of aquatic fungi that possess a reduced thallus and motile spores or gametes. In these forms the fungal thallus ranges from one to several cells which may be endobiotic or epibiotic relative to the substrate. Saccate pollen grains like those of the Pinaceae are a common food source for many of these types.

We describe here several morphological forms of aquatic fungi that occur in Pennsylvanian age cordaitean pollen grains of the genus *Sullisaccites* (*1*). We recovered the infested pollen grains from the calcium carbonate matrix of the coal ball permineralization using dilute (2 percent) hydrochloric acid (*2*). The fossil remains consist of sporangia that occur either on the surface (epibiotic) or within (endobiotic) the central body of the saccate pollen grains. In the endobiotic form the sporangia are globose and occupy the majority of the central body lumen of the pollen grain (Fig. 1, A and C). These sporangia vary from 20 to 25 μm in diameter, and, because of the presence of numerous folds in the pollen grain sporoderm, we have been unable to discern a rhizoidal system in this form. The apparent absence of specific discharge papillae may indicate that these sporangia are immature. The majority of sporangia of this type contain numerous irregularly shaped dark bodies (up to 2.5 μm in diameter) that undoubtedly represent unicellular zoospores. The preservation of such delicate structures as zoospores in rocks of Pennsylvanian age should not be regarded as unusual since numerous examples of subcellular preservation are well documented (*3*). Presumed zoospores frequently have a light refractile area centrally (Fig. 1A). The light refractile bodies within these planospores may represent the remains of oil droplets, a central vacuole, or the granules known for most aquatic motile fungi. Refractile granules are especially characteristic of zoospores in the Chytridiales (*4*).

Several forms of epibiotic sporangia also occur on pollen grains from the same sample. In one example the globose sporangium possesses several discharge papillae apically (Fig. 1E, small arrows) but contains little evidence of zoospores. The rhizoid is swollen at the base of the sporangium and resembles an irregularly shaped apophysis (Fig. 1E, large arrow). Rhizoids are approximately 3 μm in diameter, and a portion of the rhizoidal system appears to terminate at the bases of two neighboring sporangia.

A second epibiotic sporangium type is characterized by laterally located discharge papillae (Fig. 1D, arrows). In this specimen the sporangium appears to have grown out through the wall of the pollen grain air sac. In both this specimen and the epibiotic sporangium (Fig. 1B), it was not possible to locate the endobiotic rhizoidal system. It is surprising that discharge papillae are absent on the sporangium in Fig. 1B, since it contains a prominent mass of zoospores. Although exit papillae in some extant forms may not appear until shortly before spore release, it seems likely that this sporangium is an operculate type and lacks exit papillae. This form may constitute a developmental stage of the two previous types or may represent still another distinct species.

It is impossible to determine exactly the systematic relationships of these zoosporic fossil fungi. The simple morphology of the thallus is chytrid-like, but this feature is present in some members of at least five orders of extant fungi. The number and position of the zoospore flagella is the single criterion that is most important in establishing relationships among extant Phycomycetes (*5*), and we have not determined this feature for these fossils. It is also useful in extant aquatic fungi to observe the sporangium development, including formation of zoospore discharge structures, and the zoospore emergence and swimming habit. The presence or extent of a rhizoidal system is quite difficult to establish for extant fungi grown on pollen grains and has also been difficult to observe in the fossils.

Morphologically, sporangia of the endobiotic form appear holocarpic and monocentric, and they lack prominent discharge papillae. These features are characteristic of some members of the Chytridiales (Olpidiaceae), Hyphochytriales (Anisolpidiaceae), Lagenidiales (Olpidiopsidaceae, Lagenidiaceae), and Saprolegniales (Ectrogellaceae) (*6*). The epibiotic fossil forms appear to be eucarpic and either mono- or polycentric, and in this regard appear most similar to some families within the Blastocladiales

 0036-8075/78/0609-1147$00.50/0